Thermodynamic and transport investigation of $CeCoIn_{5-x}Sn_x$

E. D. Bauer,[1] F. Ronning,[1] C. Capan,[1,*] M. J. Graf,[1] D. Vandervelde,[2] H. Q. Yuan,[2] M. B. Salamon,[2] D. J. Mixson,[3] N. O. Moreno,[1,†] S. R. Brown,[4] J. D. Thompson,[1] R. Movshovich,[1] M. F. Hundley,[1] J. L. Sarrao,[1] P. G. Pagliuso,[5] and S. M. Kauzlarich[4]

[1]*Los Alamos National Laboratory, Los Alamos, New Mexico 87545, USA*
[2]*Department of Physics, University of Illinois at Urbana-Champaign, Urbana, Illinois 61801, USA*
[3]*Department of Physics, University of Florida, Gainesville, Florida 32611, USA*
[4]*Department of Chemistry, University of California, One Shields Avenue, Davis, California 95616, USA*
[5]*Cidade Universitaria, BR-13083-970 Campinas-SP, Brazil*

(Received 8 March 2006; published 16 June 2006)

Measurements of specific heat, magnetic susceptibility, electrical resistivity, and penetration depth have been performed on $CeCoIn_{5-x}Sn_x$ ($0 \leqslant x \leqslant 0.24$) single crystals. The suppression of superconductivity and the decrease of the specific heat jump at T_c, $\Delta C/T_c$, with increasing Sn concentration, and the power-law temperature dependence of penetration depth are consistent with impurity scattering calculated within the Abrikosov-Gorkov formalism indicating *d*-wave superconductivity in $CeCoIn_{5-x}Sn_x$. The non-Fermi liquid behavior [$C/T \sim -\ln T$ and $\rho(T) \sim T$] observed in the normal state in zero magnetic field is quite robust against Sn substitution (and a variety of other tuning parameters), suggesting quantum criticality involving itinerant *f*-electrons in this system.

DOI: 10.1103/PhysRevB.73.245109 PACS number(s): 71.27.+a, 72.15.Qm

I. INTRODUCTION

In *f*-electron materials, strong interactions between the localized *f* magnetic moments and the conduction electrons leads to highly correlated electron states of matter such as long-range magnetic order, magnetism coexistent with superconductivity, and a non-Fermi liquid paramagnetic ground state associated with a quantum phase transition.[1,2] Such behavior is exemplified in the $CeMIn_5$ (M=Co, Rh, Ir) heavy-fermion superconductors and, as a result, these materials have received considerable attention in recent years.[3] $CeRhIn_5$ is an antiferromagnet below $T_N=3.8$ K and undergoes a transition to a superconducting state at a pressure of ~ 10 kbar reaching a maximum transition temperature $T_c=2.1$ K at 19 kbar.[4] $CeIrIn_5$ is a heavy-fermion superconductor at ambient pressure with a bulk transition at $T_c=0.4$ K and a Sommerfeld coefficient $\gamma \sim 700$ mJ/mol K^2.[5] The application of high magnetic fields reveals a phase transition of unknown origin above $H=28$ T possibly associated with a quantum critical point (QCP).[6]

Among the $CeMIn_5$ superconductors, $CeCoIn_5$ is perhaps the most intriguing.[7] Power-law behavior found below T_c in the physical properties, such as specific heat,[8] spin lattice relaxation,[9] and thermal conductivity,[8] indicate unconventional superconductivity with line nodes of the superconducting gap on the Fermi surface. Moreover, angular-dependent thermal conductivity measurements reveal a fourfold modulation within the *ab* plane of the tetragonal crystal consistent with a *d*-wave order parameter.[10] Anomalies in the specific heat $C(T)$ and thermal conductivity $\kappa(T)$ between 10 T and the upper critical field ($H_{c2}^{ab}=12$ T) below a first-order superconducting transition $T_c \sim 0.7$ K suggest a Fulde-Ferrell-Larkin-Ovchinnikov state.[11–13]

The normal state of $CeCoIn_5$ is characterized by a *T*-linear electrical resistivity $\rho(T)$ in zero field, indicating proximity to a quantum critical point.[7,14] In magnetic fields above $H_{c2} \simeq 5$ T, ($H \| c$), a logarithmic divergence of $C(T)$ down to 50 mK, the divergence of the T^2 coefficient of $\rho(T)$, and a universal scaling of $C(H,T)$ provide strong evidence for a field-tuned QCP at $H_{QCP}=5$ T presumably associated with hidden antiferromagnetic order.[15,16] Sn substitution in $CeCoIn_5$ was used in an attempt to uncover this magnetic order by separating the upper critical field from the QCP.[17] However, for all Sn concentrations investigated, the quantum critical point could not be moved away from H_{c2}, suggesting an unusual quantum critical point associated with superconductivity. The substitution of Sn for In in $CeCoIn_5$ has been known to rapidly suppress the superconductivity.[18] This is most likely due to the preferential occupation of the Sn for the In(1) sites within the "$CeIn_3$" plane of the tetragonal structure.[19] We have therefore investigated the $CeCoIn_{5-x}Sn_x$ system by means of specific heat, electrical resistivity, magnetic susceptibility, and penetration depth in order to better understand both the effect of Sn on the superconducting properties and the nature of the quantum criticality in zero field in $CeCoIn_5$.

II. EXPERIMENTAL DETAILS

Single crystals of $CeCoIn_{5-y}Sn_y$ ($0 \leqslant y \leqslant 0.4$) were grown in In flux in the ratio Ce:Co:In:Sn=1:1:20:*y*. Magnetic measurements were performed in magnetic fields up to 5.5 T from 1.8 to 300 K using a Quantum Design SQUID (superconducting quantum interference device) magnetometer. Specific heat measurements were carried out in a Quantum Design PPMS from 0.4 to 300 K and between 0.05 and 3 K in a ^{3}He/^{4}He dilution refrigerator.

Microprobe analysis was conducted using a Cameca SX-100 electron probe microanalyzer equipped with a wavelength-dispersive spectrometer. The samples were prepared by mounting the $CeCoIn_{5-x}Sn_x$ crystals onto 25 mm

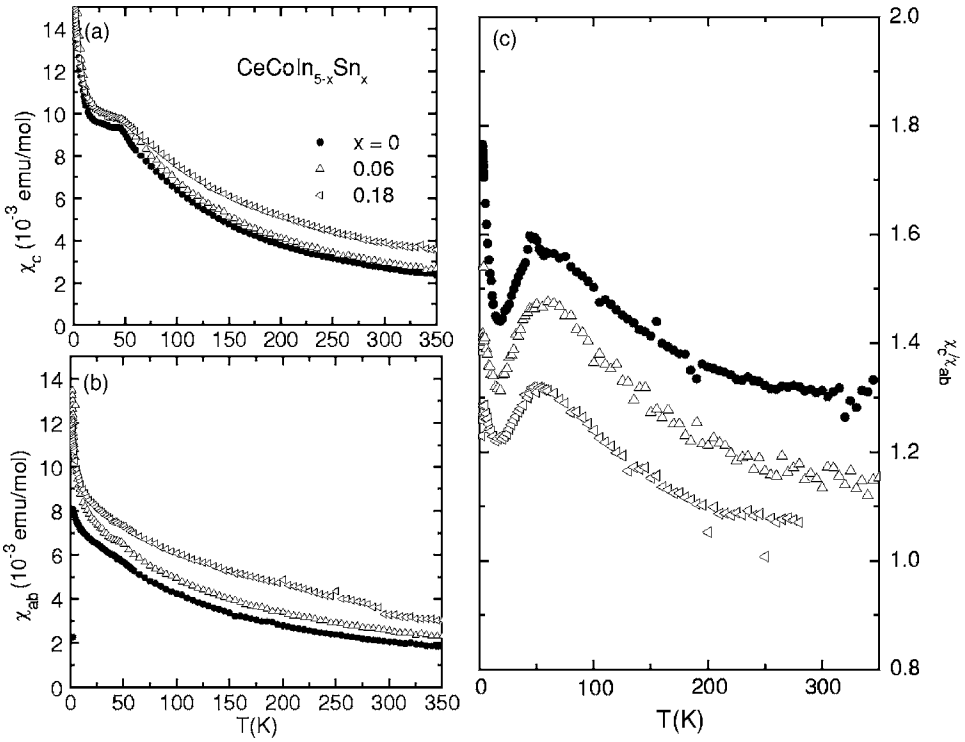

FIG. 1. Magnetic susceptibility $\chi(T)$ of $CeCoIn_{5-x}Sn_x$ measured in a magnetic field $H=0.1$ T for (a) $H\|c$ and (b) $H\|ab$ for $0\leqslant x\leqslant 0.18$. (c) Magnetic anisotropy χ_c/χ_{ab} for $0\leqslant x\leqslant 0.18$.

metal rounds by means of adhesive carbon tape. Pure Sn metal and $CeCoIn_5$ were used as standards to determine the Sn content of the doped crystals. Seven crystals were examined with nominal composition Sn=0.1, 0.15, 0.2, 0.25, 0.3, 0.35, and 0.4. Each crystal was scanned at 10–18 points along its surface with a spot size of 1 μm. The microprobe analysis reveals an actual Sn concentration of $x\sim 0.6y$; hereafter, the actual values deduced from microprobe analysis rather than the nominal values will be used.

The in-plane penetration depth measurements were performed on three concentrations of $CeCoIn_{5-x}Sn_x$, for $x=0.03$, 0.06, and 0.09. A self-inductive oscillator method was employed at 21 MHz, with noise less than one part in 10^9 and low drift. Temperature control was provided by an Oxford Kelvinox 25 dilution refrigerator that allowed temperatures down to 0.1 K. Conversion from characteristics of the system to the physical penetration depth was performed by a simple multiplication by a purely geometric factor G.[20] In this conversion, numerous approximations come into play and the margin of error is around 15%. This will not, however, affect the functional dependence of the results, only the magnitude.

III. RESULTS

A. Magnetic susceptibility

The magnetic susceptibility $\chi(T)$ for Sn concentrations $0\leqslant x\leqslant 0.18$ with $H\|ab$ and $H\|c$ is shown in Figs. 1(a) and 1(b). The overall shape and magnitude of $\chi(T)$ remains relatively unchanged with Sn substitution, implying that the crystalline electric field scheme (which presumably leads to the feature in χ_c at $\sim$50 K) is identical to that of $CeCoIn_5$.[21,22] In particular, there is only a slight monotonic increase in $\chi_{ab}(T)$ and $\chi_c(T)$, leading to a modest decrease in magnetic anisotropy χ_c/χ_{ab} of $\sim$10% [Fig. 1(c)]. Curie-Weiss fits to the data yield an effective moment close to the value expected for Ce^{3+} ($\mu_{\text{eff}}=2.54\mu_B$) and Curie-Weiss temperatures of the order $\theta_c\sim -50$ K and $\theta_{ab}\sim -100$ K, reflecting stronger antiferromagnetic correlations within the *ab* plane.

B. Specific heat

The specific heat $C(T)$ of $CeCoIn_{5-x}Sn_x$, plotted as C/T vs T for $0\leqslant x\leqslant 0.18$ is shown in Fig. 2(a). There is a monotonic decrease of both the superconducting transition and of the specific heat jump $\Delta C(T_c)$ with x. (The values of T_c and $\Delta C/T_c$ determined from an entropy conserving construction are listed in Table I and displayed in Figs. 3(a) and 3(b), respectively). Superconductivity is suppressed with increasing x at a rate $dT_c/dx=-0.6$ K/at. % Sn, about five times larger than in $Ce_{1-x}La_xCoIn_5$ ($dT_c/dx=-0.1$ K/at. % La).[23] The large specific heat jump implies that the normal state C/T must increase at low temperatures ($T<1$ K) to conserve entropy between the normal and superconducting states. The superconducting transition remains sharp for $x\leqslant 0.03$ then broadens somewhat for $x>0.03$; no superconductivity is found for $x=0.18$ above 0.4 K. The normal state value of the Sommerfeld coefficient γ at 2 K decreases only slightly with increasing x, suggesting the overall electronic structure of the Sn substituted samples remains very similar to that of $CeCoIn_5$. In the normal state, C/T exhibits a non-Fermi liquid logarithmic T dependence from $\sim$5 to 10 K down to T_c for $x\leqslant 0.15$ and to a base temperature of 0.4 K for $x=0.21$ [Fig. 2(b)] consistent with two-dimensional antiferromagnetic (AFM) spin fluctuation theories.[24,25] There is no evi-

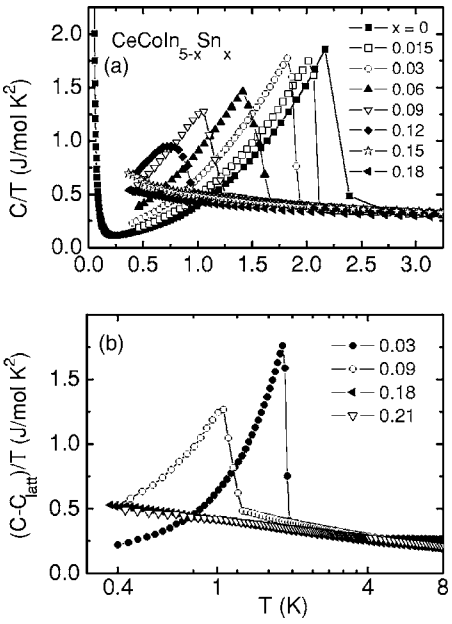

FIG. 2. (a) Specific heat C/T vs T of $CeCoIn_{5-x}Sn_x$ for $0 \leqslant x \leqslant 0.18$. (b) $(C-C_{\mathrm{latt}})/T$ vs T on a semilogarithmic scale for $0.03 \leqslant x \leqslant 0.21$. The lattice contribution of $LaCoIn_5$ has been subtracted from the data for all x.

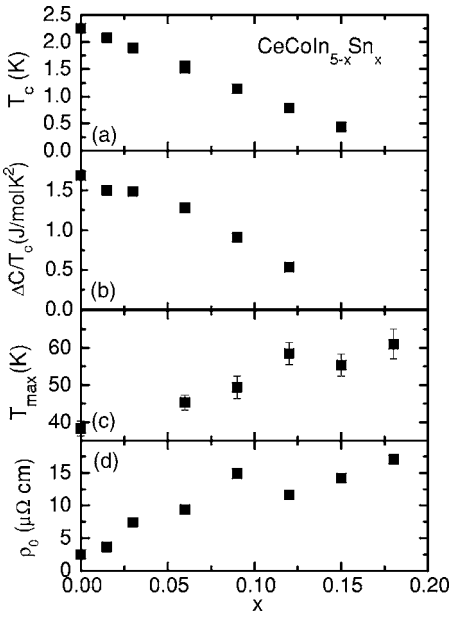

FIG. 3. Physical properties of $CeCoIn_{5-x}Sn_x$. (a) Superconducting transition temperature T_c and (b) specific heat jump at T_c, $\Delta C/T_c$, (c) temperature of maximum in electrical resistivity $T_{\max}$, and (d) residual resistivity ρ_0 vs Sn concentration x.

dence for a crossover to Fermi liquid behavior for $x \leqslant 0.24$ (above 0.4 K).

In the superconducting state, a power-law temperature dependence is observed at the lowest temperatures indicative of unconventional superconductivity in $CeCoIn_{5-x}Sn_x$ for all x as shown in Fig. 4. Taking into account a small nuclear Schottky contribution, C_{Sch}, power law fits to the data of the form

$$\frac{C - C_{\mathrm{Sch}}}{T} = \gamma_0 + BT^n \tag{1}$$

are consistent with a superconducting gap that intersects the Fermi surface along lines of nodes with an additional impurity band contribution γ_0. The exponent n increases (nearly) monotonically with increasing x, in reasonable agreement with the penetration depth measurements discussed in Sec. III D.

C. Electrical resistivity

The electrical resistivity $\rho(T)$ of $CeCoIn_{5-x}Sn_x$ is shown in Fig. 5(a) for $0 \leqslant x \leqslant 0.18$, including the nonmagnetic $LaCoIn_5$ compound. For all x, $\rho(T)$ exhibits a weak temperature dependence at higher temperatures, followed by a maximum in ρ at $T_{\max}$, before decreasing rapidly in the coherence regime. Below ~20 K, the resistivity is linear in temperature down to the superconducting transition for all Sn concentrations as displayed in Fig. 5(b) with a (near) monotonic increase in the residual resistivity ρ_0. [In some cases, the data

TABLE I. Physical properties of $CeCoIn_{5-x}Sn_x$. Superconducting transition temperature T_c; specific heat jump at T_c, ΔC; parameters γ_0 and n determined from fits of the data to Eq. (1); residual resistivity ρ_0; temperature maximum of electrical resistivity $T_{\max}$.

x	T_c (K)	$\Delta C/T_c$ $\left(\frac{\mathrm{J}}{\mathrm{mol\,K^2}}\right)$	γ_0 $\left(\frac{\mathrm{m,J}}{\mathrm{mol\,K^2}}\right)$	n	T range	ρ_0 ($\mu\Omega$ cm)	$T_{\max}$ (K)
0	2.25	1.686	40	1	0.09–0.4	2.5	38
0.015	2.08	1.497					
0.03	1.89	1.488	135	2.1	0.06–0.4	7.5	51
0.06	1.56	1.279	272	2.5	0.2–0.5	9.4	45
0.09	1.14	0.907				14.9	49
0.12	0.79	0.535	515	1.6	0.06–0.4	11.6	59
0.15	0.44	~0.1				14.2	55
0.18						17.1	61

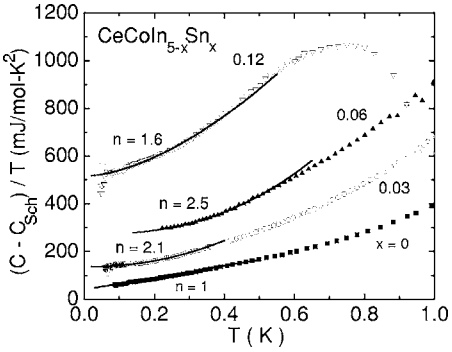

FIG. 4. Specific heat $(C-C_{\mathrm{Sch}})/T$ vs T of $CeCoIn_{5-x}Sn_x$ for $0 \leqslant x \leqslant 0.12$. A low-$T$ nuclear Schottky contribution C_{Sch} has been subtracted from the data.

can be fit to a power law $\rho(T) \sim AT^n$ with $n \sim 0.8-0.9$ over a more limited temperature range below $T \sim 5$ K; however, this slight rollover in $\rho(T)$ may be due to filaments of superconducting In in the flux-grown samples.] Both the logarithmic T dependence of C/T described above and the T-linear behavior of $\rho(T)$ suggest that $CeCoIn_{5-x}Sn_x$ is still close to a QCP for all x. After subtraction of $\rho(T)$ of $LaCoIn_5$, the temperature at which the maximum occurs in the magnetic resistivity ρ_{mag} increases with increasing x [Fig. 3(c)].

D. Penetration depth

The *ab*-plane penetration depth of $CeCoIn_{5-x}Sn_x$, plotted as $\Delta\lambda(T) \equiv \lambda(T) - \lambda_0$, is shown in Fig. 6 for $0.03 \leqslant x \leqslant 0.09$ (the transition temperatures shown in the insets of Fig. 6 are consistent with those determined from specific heat and electrical resistivity). A significant departure from the linear T

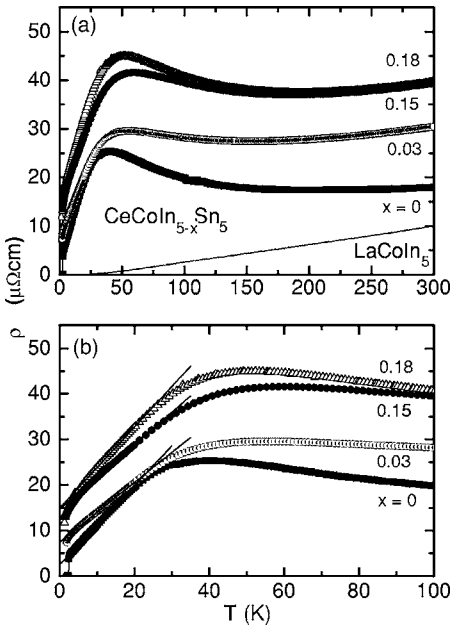

FIG. 5. (a) Electrical resistivity $\rho(T)$ of $CeCoIn_{5-x}Sn_x$ for $0 \leqslant x \leqslant 0.18$ along with $\rho(T)$ of $LaCoIn_5$ below 300 K. (b) $\rho(T)$ for $0 \leqslant x \leqslant 0.18$ below 100 K. The lines are linear fits to the data.

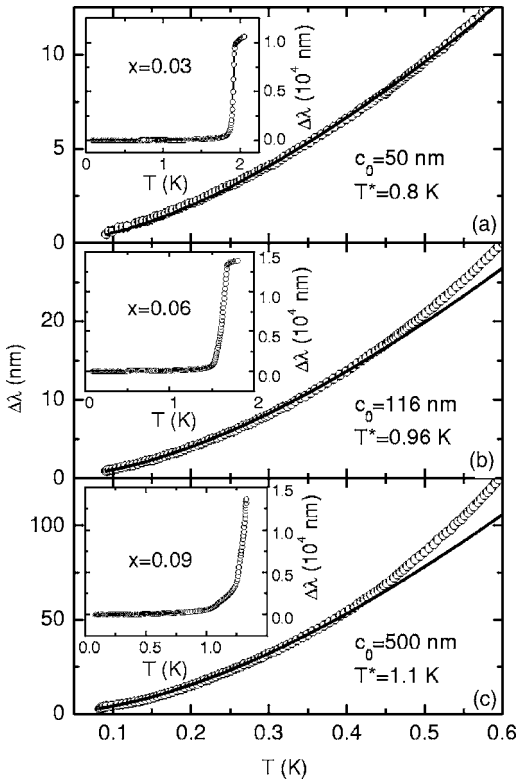

FIG. 6. Temperature dependence of penetration depth $\Delta\lambda(T)$ at low temperature for (a) $x=0.03$; (b) $x=0.06$, and (c) $x=0.09$. The solid lines are fits to the data of Eq. (2). The insets show $\Delta\lambda(T)$ over the entire temperature range.

dependence of $\Delta\lambda(T)$ in $CeCoIn_5$ (Refs. 26 and 27) is observed for all x. In three-dimensional unconventional superconductors[28] and for the particular case of two-dimensional d-wave superconductivity,[29–31] infinitesimal disorder in these unconventional superconductors with line nodes leads to a T^2 temperature dependence of the penetration depth. The disorder gives rise to a nonzero density of states at zero excitation energy and, hence, a deviation from the pure-system London penetration depth, namely, a linear temperature dependence.[32] Therefore, the model of Hirschfeld and Goldenfeld[31] that proposes a crossover at temperature T^* between these two regimes was used to fit the data. As shown in Fig. 6, the change of the penetration depth $\Delta\lambda(T)$ has been fit with the function[31]

$$\Delta\lambda(T) \equiv \lambda(T) - \lambda_0 = \frac{c_0 T^2}{T + T^*}, \tag{2}$$

where c_0 is a constant, T^* is a characteristic crossover temperature from linear ($\Delta\lambda \propto T$ for $T^* \ll T \ll T_c$) to quadratic ($\Delta\lambda \propto T^2$ for $T \ll T^* < T_c$) temperature dependence of $\Delta\lambda$, and λ_0 is the zero-temperature penetration depth. The value of T^* increases with impurity doping, in qualitative agreement with the theoretical prediction of scattering in the strong or unitary limit in which $T^* \propto \sqrt{x}$.[31] It is not possible to fit the penetration depth to a linear temperature dependence, which is consistent with a large T^*/T_c ratio of order unity. It is also noteworthy that the values of T^* in $CeCoIn_{5-x}Sn_x$

are much higher than the value reported for pure $CeCoIn_5$ ($T^*=0.3$ K).[27] The large values of T^* indicate that as impurity doping increases, scattering quickly becomes the dominant mechanism and any nonlocal thermodynamic effect, which can give rise to the same functional dependence as Eq. (2),[33] can be safely ignored; however, this conclusion is controversial for $CeCoIn_5$.[26,27] Additional measurements for different field orientations or work investigating nonlinear effects[34,35] (or the competition between nonlocal and nonlinear effects), may provide additional information in support of the topology of the nodes indicated by angle-dependent thermal conductivity[10] and specific heat measurements.[36]

IV. PAIR-BREAKING EFFECTS

Nonmagnetic impurities do not affect the transition temperature T_c in a BCS superconductor with isotropic s-wave pairing and only weakly suppress T_c for anisotropic s-wave pairing, according to Anderson's theorem for pair breaking effects in conventional superconductors.[37] However, the observed strong suppression of T_c with small amounts of Sn agrees well with the identification of $CeCoIn_5$ as an unconventional superconductor with a d-wave gap function and lines of nodes on the Fermi surface. Therefore, it is expected that a generalization of the Abrikosov-Gorkov (AG) theory to d-wave superconductivity for nonmagnetic impurities in the dilute limit is applicable and results in the implicit T_c equation[38]

$$\ln\left(\frac{T_c}{T_{c0}}\right)=\Psi\left(\frac{1}{2}\right)-\Psi\left(\frac{1}{2}+\frac{1}{2}\frac{T_{c0}}{T_c}\alpha\right), \tag{3}$$

where Ψ is the digamma function, T_{c0} is the transition temperature of the pure superconductor, and $\alpha=\hbar/(2\pi k_B T_{c0}\tau)$ is the pair-breaking parameter with lifetime τ due to elastic potential (nonmagnetic) scattering. We find that the strong suppression of the superconducting transition temperature with Sn doping is in good agreement with the generalized AG theory of pair breaking as shown in Fig. 7. The $T_c(x)$ data were fit by Eq. (3) by setting $T_{c0}=2.31$ K and writing the pair-breaking parameter as the sum of two contributions, $\alpha(x)=\alpha_0+x\beta$, where $\alpha_0=0.02$ is due to intrinsic impurities in the undoped $CeCoIn_5$ sample and $\beta=(\alpha_c-\alpha_0)/x_c=1.81$ results from elastic scattering off the Sn impurities, with a universal critical pair-breaking parameter $\alpha_c\approx 0.2807$ and corresponding critical doping value $x_c\approx 0.154$. The in-plane mean free path due to elastic scattering in the undoped $CeCoIn_5$ sample is $\ell=v_F\tau=\xi_0/\alpha_0\approx 132$ nm, with Fermi velocity $v_F=5$ km/s, while it is only $\ell\approx 9$ nm at the critical doping value x_c. For comparison, the zero-temperature superconducting coherence length, $\xi_0=\hbar v_F/2\pi k_B T_{c0}$, of the pure compound is about $\xi_0\approx 2.6$ nm, and in the Ginzburg-Landau limit $\xi\approx 5.0$ nm when determined from the slope of the upper critical field at T_c.[7] As the critical doping value x_c is approached, the mean-free path drops to $\ell=\xi_0/\alpha_c\approx 9.4$ nm, which is still 20 times the in-plane lattice constant.

The Abrikosov-Gorkov T_c suppression equation Eq. (3) is independent of the strength of the potential scatterers. On the other hand, the expression for the specific heat jump at T_c depends explicitly on it and can distinguish between weak (Born limit) and strong (unitary or resonant limit) scattering. For weak scattering, the isotropic scattering phase shift is $\delta_0\to 0$, whereas for strong scattering the phase shift is maximum, $\delta_0=\pi/2$. Our self-consistent numerical computation of the specific heat jump for arbitrary scattering strength[39,40] agrees with the analytic expression derived by Haran *et al.*[41] for d-wave superconductivity and by Ueda and Rice for unconventional heavy-fermion superconductivity[42]

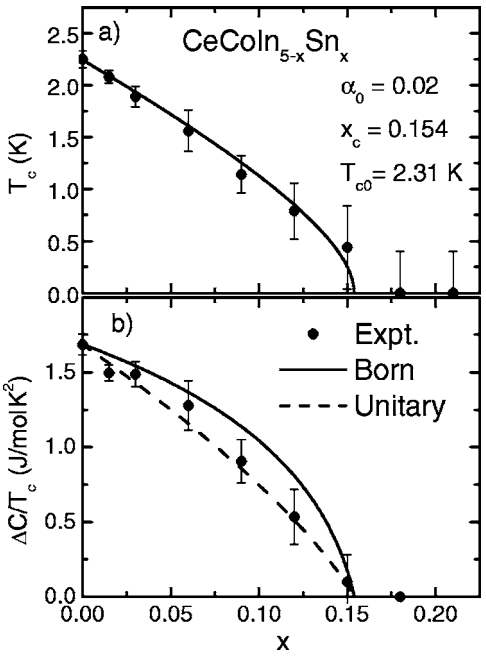

FIG. 7. (a) Superconducting transition temperature T_c vs Sn doping x of $CeCoIn_{5-x}Sn_x$ for $0\leqslant x\leqslant 0.21$. The solid line follows from the generalized AG pair-breaking formula, Eq. (3), assuming the parameters $T_{c0}=2.31$ K, $\alpha_0=0.02$, and $x_c=0.154$. The large uncertainties in measured T_c values (circles) near the critical doping x_c is largely due to the broadening of the transition. (b) Specific heat jump at T_c, $\Delta C/T_c$, vs x. The dashed (unitary limit) and solid (Born limit) lines are calculations using Eq. (4) and pair-breaking parameters and T_{c0} determined above. The theoretical heat jumps were rescaled by the experimental value at $x=0$; for a detailed discussion see Sec. IV.

$$\frac{\Delta C}{C_N(T_c)}=\frac{12\left[1-\frac{\alpha}{2}\Psi^{(1)}\left(\frac{1}{2}+\frac{\alpha}{2}\right)\right]^2}{\frac{1}{12}\frac{T_{c0}}{T_c}k\alpha\Psi^{(3)}\left(\frac{1}{2}+\frac{\alpha}{2}\right)-\frac{3}{4}\Psi^{(2)}\left(\frac{1}{2}+\frac{\alpha}{2}\right)}, \tag{4}$$

where $\Psi^{(n)}$ is the nth derivative of the digamma function, $k=\sin^2\delta_0-\cos^2\delta_0$, and the normal-state specific heat is $C_N(T)=\gamma_N T$. For a clean d-wave system ($\alpha=0$), the ratio is $\Delta C/C_N(T_c)=\Delta C/\gamma_N T_c=8/7\zeta(3)\simeq 0.9507$, where the Riemann ζ function $\zeta(3)\simeq 1.20206$. Since the measured specific heat jump of $CeCoIn_5$ is significantly larger than expected for weak-coupling s-wave superconductivity with a flat electronic density of states ($\Delta C/C_N(T_c)=1.43$),[32] we plot in Fig. 7 the dimensionless ratio of Eq. (4) multiplied by an overall scale factor (1780 mJ/mol K^2) to reproduce $\Delta C/T_c$ of the

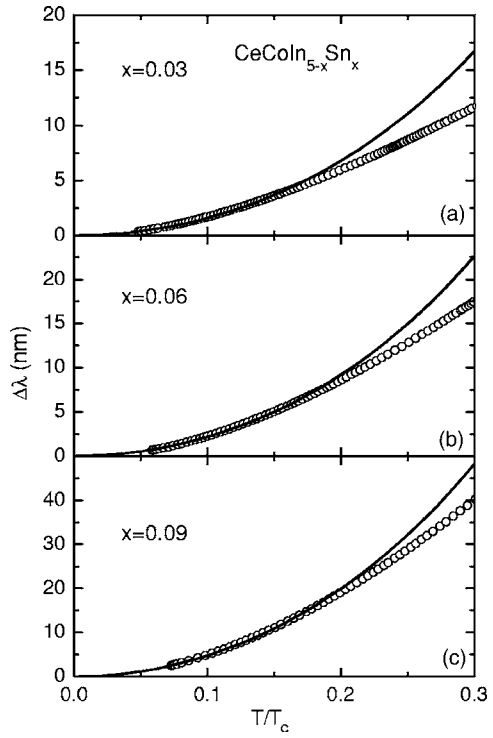

FIG. 8. Penetration depth $\Delta\lambda$ vs T/T_c for (a) $x=0.03$; (b) $x=0.06$, and (c) $x=0.09$. The solid lines are calculations based on the Abrikosov-Gorkov pair-breaking model with no adjustable parameters aside from a small correction to account for the finite temperature measurement. See Sec. IV or details.

undoped $CeCoIn_5$ sample [$\alpha=0$, compared to $\alpha=0.02$ for the measured jump (1686 mJ/mol K^2) listed in Table I]. By scaling the theoretical weak-coupling BCS value of the heat jump in Eq. (4), we crudely account for heavy-fermion or strong-coupling pairing effects manifest in the measured jump. Thus, the measured relative decrease of $\Delta C/T_c$ with increasing Sn concentration is in fairly good agreement with the theory for nonmagnetic impurity scattering in the unitary (strong scattering) limit; a result that one might expect from recent x-ray-absorption fine structure (XAFS) measurements that showed Sn preferentially occupies the In(1) site in the $CeIn_3$ planes where superconductivity is believed to develop.[19]

Next, we turn to the theoretical description of the penetration depth, or superfluid density. A standard linear response theory is used to calculate the superfluid density $\rho_s(T)\equiv 1/\lambda(T)^2$ in a weak static magnetic field for weak-coupling *d*-wave superconductivity with impurity scattering in the unitary limit.[43] By fitting the calculated $\lambda(T)=\lambda_0+\Delta\lambda(T)$ to the measured change of the penetration depth $\Delta\lambda(T)|_{\text{expt}}$ for fixed scattering rate or pair-breaking parameter α, based on our previous analysis of T_c suppression and specific heat jump, we deduce the zero-temperature penetration depth $\lambda_0(x)$. Since the base temperature of the $\Delta\lambda(T)|_{\text{expt}}$ measurements was about 0.1 K, a small correction to $\Delta\lambda(T)|_{\text{expt}}$ is allowed for when comparing to the theoretical change of λ from absolute zero temperature. As shown in Fig. 8, reasonable agreement between theoretical fits and the data is found below $T/T_c<0.2$. The values of the fitted zero-temperature penetration depths,[52] $\lambda_0=332,485,1050$ nm for $x=0.03,0.06,0.09$, are of reasonable size compared to pure $CeCoIn_5$ [$\lambda_0=281$ nm (Ref. 27), $\lambda_0=550$ nm (Ref. 44).] For small scattering rate and narrow impurity band $\varepsilon^*\ll\Delta_0$, there is a simple relationship between the crossover temperature and doping,[31]

$$T^* \sim 1.32\varepsilon^* \approx 0.47\sqrt{\alpha(x)T_c(x=0)\Delta_0}. \quad (5)$$

The theoretical crossover temperatures are $T^*=0.45,0.59,0.70$ K for $x=0.03,0.06,0.09$, respectively. As expected, the clean limit formula [Eq. (5)] consistently underestimates the experimentally determined T^* by roughly 50%; see Fig. 6. Also note that the increase of λ_0 with Sn concentration is much stronger than the *d*-wave model predicts for impurity scattering in the unitary limit. Although the "dirty" *d*-wave model results in fair agreement with the low-temperature penetration depth in $CeCoIn_{5-x}Sn_x$, it falls short of accounting for the significant increase of the measured zero-temperature penetration depth λ_0 with x. This shortcoming may be attributed to strong-coupling effects as indicated by an enhanced gap ratio $2\Delta/k_BT_c=4.64$,[45] or to electronic correlations similar to Fermi-liquid effects, or to inelastic scattering from antiferromagnetic spin fluctuations as speculated above for the doping dependence of the residual Sommerfeld coefficient γ_0 of the specific heat in the superconducting state.

V. DISCUSSION

The non-Fermi liquid (NFL) normal state in $CeCoIn_5$ is remarkably robust when subjected to a variety of external tuning parameters, such as pressure, magnetic field, and chemical substitution, and may be related to the partial itineracy of the *f*-electrons in this material. Sn substitution has little effect on the normal state properties; both the NFL behavior in $C(T)$ and $\rho(T)$ associated with proximity to a quantum critical point, is still observed in all the $CeCoIn_{5-x}Sn_x$ samples investigated ($x\leqslant 0.24$). In pure $CeCoIn_5$, the application of magnetic fields reveals non-Fermi liquid behavior in specific heat and electrical resistivity above the upper critical field $H_{c2}=4.95$ T ($H\|c$); furthermore, universal scaling of $C(H,T)$ indicates a field-tuned QCP at $H_{QCP}=5$ T associated with hidden magnetic order that resides within the dome of superconductivity.[15] Similar behavior is found when the field is applied within the *ab* plane where $H_{c2}=12$ T.[46] Measurements in magnetic fields on $CeCoIn_{5-x}Sn_x$ ($x\leqslant 0.12$) reveal nearly identical $H-T$ phase diagrams for all Sn concentrations (aside from a decrease in H_{c2}), suggesting that the field-tuned QCP is intimately linked to superconductivity.[17] These experiments could not distinguish whether the quantum criticality in $CeCoIn_{5-x}Sn_x$ in magnetic field is associated with a superconducting quantum critical point or if field-suppressed magnetic order masked by superconductivity gives rise to such NFL behavior. In any case, it appears that the Ce *f*-electrons in $CeCoIn_{5-x}Sn_x$ are quantum critical over quite a large region of $H-T-x$ phase space. This is illustrated in Fig. 9, where there is an extended NFL regime both above H_{c2} and in zero field above T_c.

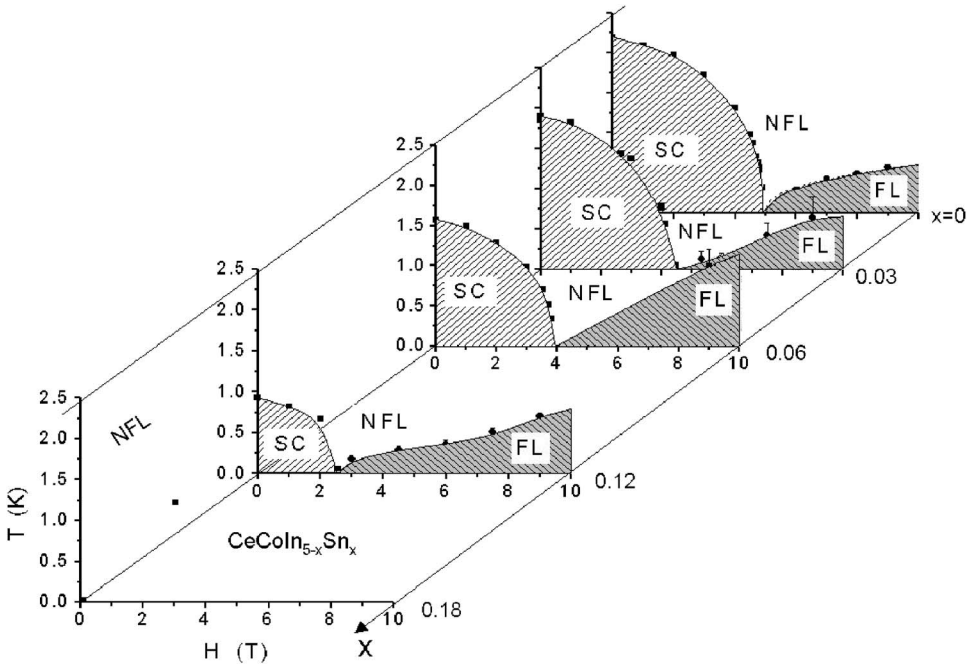

FIG. 9. Composition-magnetic field-temperature ($x-H-T$) phase diagram of $CeCoIn_{5-x}Sn_x$ ($0 \leqslant x \leqslant 0.18$). SC-superconducting, NFL-non-Fermi liquid, and FL-Fermi liquid. Data from this work and Ref. 17.

A simple argument for this robust NFL behavior in $CeCoIn_{5-x}Sn_x$ is described as follows. Pressure measurements[14] on $CeCoIn_5$ indicate this material is located just beyond a slightly negative pressure antiferromagnetic quantum critical point, the only remnants being the unconventional superconductivity and the NFL normal state at ambient pressure. In analogy to the large change in Fermi surface volume in $CeRhIn_5$ at the AFM QCP ($P_c \sim 25$ kbar) discussed below,[47] $CeCoIn_5$ resides just on the positive pressure (itinerant) side of a localized-itinerant crossover of the Ce $4f$ electrons. Sn substitution for In in $CeCoIn_5$ should increase the hybridization of the local moment and conduction electron states with little or no change in the Fermi surface volume (there is no detectable change in the lattice parameters in $CeCoIn_{5-x}Sn_x$ from x-ray diffraction). Substitution of Sn for In in $CeIn_{3-y}Sn_y$ also increases the hybridization, but in contrast to $CeCoIn_{5-x}Sn_x$, increasing y also expands the unit cell (e.g., acts as a negative pressure).[48] To the extent that Sn primarily occupies the planar In(1) site in $CeCoIn_{5-x}Sn_x$, i.e., is similar to $CeIn_{3-y}Sn_y$, then the balance between competing tendencies for the $4f$ electrons to remain (partially) localized (no change in unit cell volume) but hybridize more strongly with increasing x may provide an explanation of the insensitivity of the electronic specific heat and the prevalence of the NFL properties in $CeCoIn_{5-x}Sn_x$. A potential difficulty with this simple picture is the 50% increase in $T_{\max}$ with increasing Sn concentration, implying that the two competing effects are, in fact, not perfectly balanced. However, a "two-fluid" description[49] of the electrical resistivity and specific heat may resolve this apparent discrepancy. In this model, $\rho(T)$ is the product of a noninteracting "Kondo impurity" resistivity and the time-averaged fraction of these impurities, $1-F(T)$, where $F(T)$ is the fraction of f-electron degrees of freedom that assume itinerant character that dominate at low T. As the temperature is lowered $F(T)$ increases, leading to a maximum in the electrical resistivity at $T_{\max}$ close to the temperature where intersite coupling begins to dominate. The specific heat can also be decomposed in a similar manner. In $CeCoIn_5$, $F(T)$ increases linearly from 0 at $T \sim 45$ K to $F(T_c) \simeq 0.9$. If the F function increases with increasing x with a nearly identical slope $\Delta F/\Delta T$ to that of pure $CeCoIn_5$ (consistent with the entropy balance of the normal and superconducting states), then the near equality of the Sommerfeld coefficient between $x=0$ and $x=0.18$ implies that the low-T properties remain virtually unaffected; in other words, the change in $\Delta F/\Delta T$ caused by the increase in hybridization are insignificant below 2 K. For example, assuming that the NFL ground state of the $x=0.18$ sample also gives $F(0)=1$, the difference in slopes due to an increase in $T_{\max}$ of 20 K between $CeCoIn_5$ [$\Delta F/\Delta T \simeq 0.021$ K^{-1} (Ref. 49)] and $x=0.18$ ($\Delta F/\Delta T \simeq 0.017$ K^{-1}) leads to a small change of a few percent in γ that is within our uncertainties in the measurement.

Pressure has the greatest influence on the quantum critical point at zero field and the field-tuned QCP in $CeCoIn_5$. The non-Fermi liquid linear T dependence in $\rho(T)$ evolves into a Fermi liquid regime above $P=16$ kbar coincidentally after a maximum is reached in the superconducting transition temperature. Recent electrical resistivity measurements on $CeCoIn_5$ under pressure and in applied magnetic fields reveal a separation of the field-tuned QCP from H_{c2} [deduced from the decreased divergence of the T^2 coefficient of $\rho(H,T)$] upon approaching the upper critical field at applied pressures above 10 kbar.[50] These results indicate the field-induced NFL behavior near H_{c2} at ambient pressure is not associated with a superconducting QCP, but instead may be related to the suppression of long-range magnetic order hidden within the superconducting state; at the very least, they suggest that the combination of pressure- and magnetic-field tuning[50] is quite different from field tuning alone.[15]

Recent de Haas van Alphen (dHvA) experiments performed under pressure on $CeRhIn_5$ reveal a divergence of the

effective mass close to P_c consistent with proximity to an antiferromagnetic QCP. The change in the Fermi surface volume deduced from the shift in the dHvA frequencies has been interpreted as a localized-itinerant crossover of the $4f$ electrons upon crossing the QCP. What is remarkable is that the dHvA frequencies above P_c in $CeRhIn_5$ closely resemble those of $CeCoIn_5$ at ambient pressure; thus, the quantum criticality observed in $CeRhIn_5$ at P_c occurs where the f-electron degrees of freedom become very similar to itinerant $CeCoIn_5$. (Band structure calculations on $CeCoIn_5$ assuming the Ce $4f$ electrons are itinerant, consistent with dHvA measurements, support this idea.[51]) Therefore, we conjecture that the robustness of the NFL behavior found in $CeCoIn_5$ when the system is tuned by Sn substitution, magnetic field, pressure, or a combination thereof, may be related to the partial itineracy of the f-electrons in this material.

VI. CONCLUSION

In summary, measurements of specific heat, magnetic susceptibility, electrical resistivity, and penetration depth have been performed on single crystals of $CeCoIn_{5-x}Sn_x$ ($0 \leqslant x \leqslant 0.24$). The pair-breaking effects on the superconducting properties, such as $T_c(x)$, $\Delta C/T_c$, and $\Delta\lambda(x,T)$, calculated within an extended Abrikosov-Gorkov formalism are consistent with d-wave superconductivity for all x. The NFL behavior that persists over a wide range of phase space is suggested to arise from itinerant f-electrons in $CeCoIn_{5-x}Sn_x$.

ACKNOWLEDGMENTS

We thank M. B. Maple for useful discussions. Work at Los Alamos was performed under the auspices of the U.S. DOE. Work at UC-Davis was funded by the NSF.

*Present address: Department of Physics, and Astronomy, Louisiana State University, Baton Rouge, Louisiana 70802 USA

†Present address: Department of Physics, Federal University of Sergipe, Sao Cristovao, SE 49100-000, Brazil

[1] M. B. Maple, Physica B **215**, 110 (1995).

[2] G. R. Stewart, Rev. Mod. Phys. **73**, 797 (2001).

[3] J. D. Thompson, M. Nicklas, A. Bianchi, R. Movshovich, A. Llobet, W. Bao, A. Malinowski, M. F. Hundley, N. O. Moreno, P. G. Pagliuso, J. L. Sarrao, S. Nakatsuki, Z. Fisk, R. Borth, E. Lengyel, N. Oeschler, G. Sparn, and F. Stehlich, Physica B **329**, 446 (2003).

[4] H. Hegger, C. Petrovic, E. G. Moshopoulou, M. F. Hundley, J. L. Sarrao, Z. Fisk, and J. D. Thompson, Phys. Rev. Lett. **84**, 4986 (2000).

[5] C. Petrovic, R. Movshovich, M. Jaime, P. G. Pagliuso, M. F. Hundley, J. L. Sarrao, Z. Fisk, and J. D. Thompson, Europhys. Lett. **53**, 354 (2001).

[6] J. S. Kim, J. Alwood, P. Kumar, and G. R. Stewart, Phys. Rev. B **65**, 174520 (2002).

[7] C. Petrovic, P. G. Pagliuso, M. F. Hundley, R. Movshovich, J. L. Sarrao, J. D. Thompson, Z. Fisk, and P. Monthoux, J. Phys.: Condens. Matter **13**, L337 (2001).

[8] R. Movshovich, M. Jaime, J. D. Thompson, C. Petrovic, Z. Fisk, P. G. Pagliuso, and J. L. Sarrao, Phys. Rev. Lett. **86**, 5152 (2001).

[9] Y. Kohori, Y. Yamato, Y. Iwamoto, T. Kohara, E. D. Bauer, M. B. Maple, and J. L. Sarrao, Phys. Rev. B **64**, 134526 (2001).

[10] K. Izawa, H. Yamaguchi, Y. Matsuda, H. Shishido, R. Settai, and Y. Ōnuki, Phys. Rev. Lett. **87**, 057002 (2001).

[11] A. Bianchi, R. Movshovich, C. Capan, P. G. Pagliuso, and J. L. Sarrao, Phys. Rev. Lett. **91**, 187004 (2003).

[12] H. A. Radovan, N. A. Fortune, T. P. Murphy, S. T. Hannahs, E. C. Palm, S. W. Tozer, and D. Hall, Nature (London) **425**, 51 (2003).

[13] P. Fulde and R. A. Ferrell, Phys. Rev. **135**, A550 (1964); A. J. Larkin, and Y. N. Ovchinnikov, Sov. Phys. JETP **20**, 762 (1965).

[14] V. A. Sidorov, M. Nicklas, P. G. Pagliuso, J. L. Sarrao, Y. Bang, A. V. Balatsky, and J. D. Thompson, Phys. Rev. Lett. **89**, 157004 (2002).

[15] A. Bianchi, R. Movshovich, I. Vekhter, P. G. Pagliuso, and J. L. Sarrao, Phys. Rev. Lett. **91**, 257001 (2003).

[16] J. Paglione, M. A. Tanatar, D. G. Hawthorn, E. Boaknin, R. W. Hill, F. Ronning, M. Sutherland, L. Taillefer, C. Petrovic, and P. C. Canfield, Phys. Rev. Lett. **91**, 246405 (2003).

[17] E. D. Bauer, C. Capan, F. Ronning, R. Movshovich, J. D. Thompson, and J. L. Sarrao, Phys. Rev. Lett. **94**, 047001 (2005).

[18] E. D. Bauer, N. O. Moreno, D. J. Mixson, J. L. Sarrao, J. D. Thompson, M. F. Hundley, R. Movshovich, and P. G. Pagliuso, Physica B **359-61**, 35 (2005).

[19] M. Daniel, E. D. Bauer, S.-W. Han, C. H. Booth, A. L. Cornelius, P. G. Pagliuso, and J. L. Sarrao, Phys. Rev. Lett. **95**, 016406 (2005).

[20] E. E. M. Chia, M. B. Salamon, H. Sugawara, and H. Sato, Phys. Rev. Lett. **91**, 247003 (2003).

[21] E. D. Bauer, A. D. Christianson, J. M. Lawrence, E. A. Goremychkin, N. O. Moreno, N. J. Curro, F. R. Trouw, J. L. Sarrao, J. D. Thompson, R. J. McQueeney, W. Bao, and R. Osborn, J. Appl. Phys. **95**, 7201 (2004).

[22] A. D. Christianson, E. D. Bauer, J. M. Lawrence, P. S. Riseborough, N. O. Moreno, P. G. Pagliuso, J. L. Sarrao, J. D. Thompson, E. A. Goremychkin, F. R. Trouw, M. P. Hehlen, and R. J. McQueeney, Phys. Rev. B **70**, 134505 (2004).

[23] S. Nakatsuji, S. Yeo, L. Balicas, Z. Fisk, P. Schlottmann, P. G. Pagliuso, N. O. Moreno, J. L. Sarrao, and J. D. Thompson, Phys. Rev. Lett. **89**, 106402 (2002).

[24] J. A. Hertz, Phys. Rev. B **14**, 1165 (1976).

[25] T. Moriya and T. Takimoto, J. Phys. Soc. Jpn. **64**, 960 (1995), and refs. therein.

[26] E. E. M. Chia, D. J. Van Harlingen, M. B. Salamon, B. D. Yanoff, I. Bonalde, and J. L. Sarrao, Phys. Rev. B **67**, 014527 (2003).

[27] S. Özcan, D. M. Broun, B. Morgan, R. K. W. Haselwimmer, J. L. Sarrao, S. Kamal, C. P. Bidinosti, P. J. Turner, M. Raudsepp, and J. R. Waldram, Europhys. Lett. **62**, 412 (2003).

[28] D. Einzel, P. J. Hirschfeld, F. Gross, B. S. Chandrasekhar, K. Andres, H. R. Ott, J. Beuers, Z. Fisk, and J. L. Smith, Phys. Rev.

Lett. **56**, 2513 (1986).
[29] M. Prohammer and J. P. Carbotte, Phys. Rev. B **43**, 5370 (1991).
[30] P. Arberg, M. Mansor, and J. P. Carbotte, Solid State Commun. **86**, 671 (1993).
[31] P. J. Hirschfeld and N. Goldenfeld, Phys. Rev. B **48**, 4219 (1993).
[32] See, for example, M. Tinkham, *Introduction to Superconductivity* (McGraw-Hill, New York, 1975).
[33] I. Kosztin and A. J. Leggett, Phys. Rev. Lett. **79**, 135 (1997).
[34] S.-K. Yip and J. A. Sauls, Phys. Rev. Lett. **69**, 2264 (1992).
[35] D. Xu, S.-K. Yip, and J. A. Sauls, Phys. Rev. B **51**, 16233 (1995).
[36] H. Aoki, T. Sakakibara, H. Shishido, R. Settai, Y. Onuki, P. Miranovic, and K. Machida, J. Phys.: Condens. Matter **16**, L13 (2004).
[37] P. W. Anderson, Phys. Rev. Lett. **3**, 325 (1959).
[38] L. P. Gorkov, Sov. Sci. Rev., Sect. A **A9**, 1 (1987).
[39] M. J. Graf and A. V. Balatsky, Phys. Rev. B **62**, 9697 (2000).
[40] M. J. Graf, S.-K. Yip, and J. A. Sauls, Phys. Rev. B **62**, 14393 (2000).
[41] G. Haran, J. Taylor, and A. D. S. Nagi, Phys. Rev. B **55**, 11778 (1997).
[42] K. Ueda and T. M. Rice, in *Theory of Heavy Fermions and Valence Fluctuations*, edited by T. Kasuya and T. Saso (Springer, New York, 1985), p. 267.
[43] C. H. Choi and P. Muzikar, Phys. Rev. B **39**, 11296 (1989).
[44] W. Higemoto, A. Koda, R. Kadano, Y. Kawasaki, Y. Haga, D. Aoki, R. Settai, H. Shishido, and Y. Onuki, J. Phys. Soc. Jpn. **71**, 1023 (2002).
[45] W. K. Park, L. H. Greene, J. L. Sarrao, and J. D. Thompson, Phys. Rev. B **72**, 052509 (2005).
[46] F. Ronning, C. Capan, A. Bianchi, R. Movshovich, A. Lacerda, M. F. Hundley, J. D. Thompson, P. G. Pagliuso, and J. L. Sarrao, Phys. Rev. B **71**, 104528 (2005).
[47] H. Shishido, R. Settai, H. Harima, and Y. Onuki, J. Phys. Soc. Jpn. **74**, 1103 (2005).
[48] J. G. Sereni, Physica B **215**, 273 (1995).
[49] S. Nakatsuji, D. Pines, and Z. Fisk, Phys. Rev. Lett. **92**, 016401 (2004).
[50] F. Ronning, C. Capan, E. D. Bauer, J. D. Thompson, J. L. Sarrao, and R. Movshovich, Phys. Rev. B **73**, 064519 (2006)
[51] H. Shishido, R. Settai, D. Aoki, S. Ikeda, H. Nakawaki, N. Nakamura, T. Iizuka, Y. Inada, K. Sugiyama, T. Takeuchi, K. Kindo, T. C. Kobayashi, Y. Haga, H. Harima, Y. Aoki, T. Namiki, H. Sato, and Y. Ōnuki, J. Phys. Soc. Jpn. **71**, 162 (2002).
[52] Better fits to the low-temperature $\lambda(T)$ data between $0 < T/T_c < 0.3$ are obtained with the pair-breaking parameter as an additional fit parameter. Such fits result in values of λ_0 about one-third smaller than those listed in Sec. IV because of the smaller α as $T \rightarrow 0$.